Self-Consistent Supercell Band-Structure Calculations for the Investigation of the Electric Field Gradient at Impurity Sites in Cd Metal

P. C. Schmidt and Al. Weiss
Institut für Physikalische Chemie, Physikalische Chemie III, Technische Hochschule Darmstadt

S. Cabus and J. Kübler
Institut für Festkörperphysik, Technische Hochschule Darmstadt*

Z. Naturforsch. **42a**, 1321–1326 (1987); received August 31, 1987

Dedicated to Prof. Dr. K. G. Weil on the Occasion of his 60th Birthday

The electric field gradient (EFG) at the nuclei of the 5 sp impurities In, Sn, Sb, I and Xe in Cd metal is investigated on the basis of supercell band structure calculations of $Cd_{15}M$ (M = In, ..., Xe). The theoretical results show the same trend as the experimental findings. The differences in the EFG for different impurities are related to the charge distribution and partial densities of states.

1. Introduction

Nuclear quadrupole interaction data in metallic systems with various kinds of point defects are available for a large number of metallic systems (for references see e.g. [1, 2]). The theoretical understanding of the origin of the electric field gradient (EFG) has been of great interest, especially for those systems, for which the sign of the EFG has been measured. It is found that the EFG of the substitutional impurities In to Xe in Cd metal at the site of the impurity is positive for metal – and negative for non-metal impurities. The origin of the sign reversal was studied before by a tight-binding model [3] and by molecular-cluster calculations [4]. To adjust the molecular picture to impurities in the solid certain assumptions had to be made about the spectral distribution of the electronic states in the crystal. Within the tight-binding model, functions of Gaussian type were used to get the partial densities of states (spectral distribution of the p-like states) [3], whereas in the cluster investigations an approximately free- electron type of density-of-states with some structure was used [4]. In the present work the EFG and the (partial) densities of states in these systems is obtained from self-consistent, solid-state band-structure calculations. The electronic structure of Cd metal with a substitutional point impurity is simulated by the electronic states calculated for a crystal containing 15 Cd atoms and one impurity atom in the unit cell. Our investigations show the role of a) the filling-up of electronic states of different $p_x = p_y$ and p_z amplitudes and b) the local electronic properties of the impurity atom on the magnitude and sign of the EFG.

2. Theoretical Background

The EFG, q, representing the maximum component in the principal axis system (along the c axis in the metallic systems considered here) is given by

$$q = q_{c,d}(1 - \gamma_\infty) + q_{v,d} + q_{v,s}, \tag{1}$$

where

$$q_{c,d} = \sum_v \frac{Z_v}{4\pi\varepsilon_0} \frac{3\cos^2\vartheta_v - 1}{r^3}; \tag{2}$$

$$q_{v,d} = -\frac{e}{4\pi\varepsilon_0} \int (3\cos^2\vartheta - 1)\, r^{-3}\, \varrho(\boldsymbol{r})\, d\tau; \tag{3}$$

$$q_{v,s} = \frac{e}{4\pi\varepsilon_0} \int \gamma(r)\,(3\cos^2\vartheta - 1)\, r^{-3}\, \varrho(\boldsymbol{r})\, d\tau. \tag{4}$$

$q_{c,d}$ and $q_{v,d}$ are the direct contributions from the ionic cores of charges Z_v at site v and the valence electrons of charge density $\varrho(\boldsymbol{r})$, respectively. Within perturbation theory γ_∞ and $\gamma(r)$ take into account the distortion of the electronic cores by the non spherically symmetric environment. γ_∞ is the Sternheimer antishielding factor [5] for the ions in the lattice appropri-

* Hochschulstraße 2, D-6100 Darmstadt.

Reprint requests to Priv.-Doz. Dr. P. C. Schmidt, Institut für Physikalische Chemie, Technische Hochschule Darmstadt, Petersenstr. 20, D-6100 Darmstadt, West Germany.

0932-0784 / 87 / 1100-1321 $ 01.30/0. – Please order a reprint rather than making your own copy.

Dieses Werk wurde im Jahr 2013 vom Verlag Zeitschrift für Naturforschung in Zusammenarbeit mit der Max-Planck-Gesellschaft zur Förderung der Wissenschaften e.V. digitalisiert und unter folgender Lizenz veröffentlicht: Creative Commons Namensnennung-Keine Bearbeitung 3.0 Deutschland Lizenz.

This work has been digitalized and published in 2013 by Verlag Zeitschrift für Naturforschung in cooperation with the Max Planck Society for the Advancement of Science under a Creative Commons Attribution-NoDerivs 3.0 Germany License.

Zum 01.01.2015 ist eine Anpassung der Lizenzbedingungen (Entfall der Creative Commons Lizenzbedingung „Keine Bearbeitung") beabsichtigt, um eine Nachnutzung auch im Rahmen zukünftiger wissenschaftlicher Nutzungsformen zu ermöglichen.

On 01.01.2015 it is planned to change the License Conditions (the removal of the Creative Commons License condition "no derivative works"). This is to allow reuse in the area of future scientific usage.

ate for the EFG due to the totally external charge, and $\gamma(r)$ is the antishielding function [6] which depends on the distance r of the valence electron from the nucleus.

To get some insight into the order of magnitude of the different contributions to the EFG we first give theoretical results for pure Cd metal.

The direct contribution $q_{c,d}$ can be determined from a lattice sum calculation [7]. For Cd metal one obtains [8] $q_{c,d} = -0.11 \cdot 10^{17}\,\mathrm{V/cm^2}$.

Using an antishielding factor for Cd^{2+} of -31.9 [8] one obtains the total core contribution in pure Cd metal [8] to be $q_c = q_{c,d}(1-\gamma_\infty) = -3.57 \cdot 10^{17}\,\mathrm{V/cm^2}$.

The valence electron contribution $q_{v,d}$ is calculated using the orthogonalized plane-wave (OPW) procedure [2, 8] to be $q_{v,d} = 8.73 \cdot 10^{17}\,\mathrm{V/cm^2}$ or, using the linearized augmented plane-wave method [9] $q_{v,d} = 8.31 \cdot 10^{17}\,\mathrm{V/cm^2}$. The difference between the two values is caused by the choice of different procedures and by slightly different c/a ratios used for these calculations.

A first-principles determination of the shielding of the valence electrons is still rather difficult; therefore we use the value from an OPW calculation, which gives approximately [8] $q_{v,s} = 3.84 \cdot 10^{17}\,\mathrm{V/cm^2}$. One sees that this shielding contribution nearly cancels the shielding contribution of the atomic cores, see above.

It follows that the total EFG is nearly equal to $q_{v,d}$. This finding also follows from self-consistent calculations [4, 9], where the shielding effects are incorporated in the self-consistent procedure rather than calculated by perturbation theory. It seems that the valence electron contribution $q_{v,d}$ is the dominant contribution to the total EFG and, therefore, to study trends in the systems Cd-M, M = In, ..., Xe, only this contribution is considered in the following.

Next we briefly outline how the theoretical expression for $q_{v,d}$ can be simplified.

In the effective-one-particle model the electron density in (3) is given by summing the square of the one-electron wave- functions ψ_i over all occupied states i

$$\varrho(\boldsymbol{r}) = \sum_{i}^{\mathrm{occ.}} |\psi_i(\boldsymbol{r})|^2 . \tag{5}$$

In the present work the wave-functions ψ_i are calculated by the augmented spherical wave (ASW) procedure [10]. One aspect of this procedure is that the crystal is separated into overlapping atomic spheres. The sizes of the atomic spheres are chosen in such a way that the volume of the spheres is equal to the crystal volume (Wigner-Seitz spheres). For our calculations the radii of the Wigner-Seitz spheres are all equal to 1.714 Å. The crystal potential is approximated by its spherical symmetric contribution. Inside the spheres the angular part of the wave-functions is expanded in spherical harmonics times numerical solutions of the radial Schrödinger equation with boundary conditions that match differentially to spherical waves.

In a simplified way the ψ_i inside the atomic spheres can be written as

$$\psi_i^{(v)} = \sum_L a_{L,i}^{(v)} R_{l,i}^{(v)}(r)\, Y_L(\vartheta, \varphi), \tag{6}$$

where the Y_L are the spherical harmonics with $L = (l, m_l)$, the $R_{l,i}^{(v)}(r)$ are the radial wave functions and the $a_{L,i}^{(v)}$ are coefficients calculated by the self-consistent procedure. For the EFG at the nuleus v, (3), one gets within this approximation

$$q_{v,d}^{(v)} = \sum_{i}^{\mathrm{occ.}} \sum_{L,L'} q_i^{(v)}(L, L'), \tag{7}$$

where

$$q_i^{(v)}(L, L') = a_{L,i}^{(v)}\, a_{L',i}^{(v)*}\, I_{i,l,l'}^{(v)}\, C_{L,L'} ; \tag{8}$$

$$C_{L,L'} = \int Y_L(\vartheta, \varphi)\, Y_{L'}^*(\vartheta, \varphi)(3\cos^2\vartheta - 1)\,\mathrm{d}\Omega ; \tag{9}$$

$$I_{i,l,l'}^{(v)} = \int R_{l,i}^{(v)}(r)\, R_{l',i}^{(v)}(r)\, r^{-1}\,\mathrm{d}r . \tag{10}$$

For the systems considered here it is found that the dominant terms of $q_i^{(v)}(L, L')$ are the three contributions $q_i^{(v)}(p_x, p_x) = q_i^{(v)}(p_x)$, $q_i^{(v)}(p_y, p_y) = q_i^{(v)}(p_y)$ and $q_i^{(v)}(p_z, p_z) = q_i^{(v)}(p_z)$. Taking the average of $I_{i,p,p}^{(v)}$ $(= \langle r^{-3}\rangle_v)$ and noticing that $C_{p_x,p_x} = C_{p_y,p_y} = -\frac{2}{5}$, $C_{p_z,p_z} = \frac{4}{5}$, one gets approximately

$$q_{v,d}^{(v)} \approx \tfrac{4}{5}\langle r^{-3}\rangle_v (Q_{p_x}^{(v)} - Q_{p_z}^{(v)}) \tag{11}$$

with

$$Q_{p_j}^{(v)} = \sum_{i}^{\mathrm{occ.}} |a_{L,i}^{(v)}|^2 . \tag{12}$$

Equation (11) looks similar to corresponding molecular expressions [11]. If the $R_{l,i}^{(v)}(r)$ are normalized in the Wigner-Seitz sphere, $Q_{p_j}^{(v)}$ is equal to the total amount of p_j-like charge of the wave functions inside the atomic sphere v.

To study the trends in the EFG at the nuclei of various impurities it is helpful to introduce the concept of partial density of states $N_v(E)$. $N_v(E)$ are the density of states $N(E)$ weighted by the norms of the wave functions inside the atomic sphere such that

$$Q_v = \int_0^{E_F} N_v(E)\,\mathrm{d}E , \tag{13}$$

where E_F is the Fermi energy, and where the charge inside the overlapping regions and inside the interstitial region is distributed over the different atomic spheres [10].

Since the wave functions are expanded in spherical harmonics, $N_v(E)$ can be separated into L dependent components $N_{v,L}(E)$:

$$N_v(E) = \sum_L N_{v,L}(E) \tag{14}$$

The $N_{v,L}(E)$ are the L-partial densities of states. For the hcp lattice $N_{v,p_x}(E) = N_{v,p_y}(E)$, and (11) can be written as

$$q_{v,d}^{(v)} \approx \tfrac{4}{5} \langle r^{-3} \rangle_v [Q_{v,p_x}(E_F) - Q_{v,p_z}(E_F)], \tag{15}$$

$$Q_{v,p_j}(E) = \int_0^{E_F} N_{v,p_j}(E')\, dE' . \tag{16}$$

From (15) and (16) one sees that the sign of the EFG depends on the spectral distribution of the p_j-like charge. For the Cd-M alloys $N_{v,p_j}(E)$ and $Q_{v,p_j}(E)$ are given in the next section.

3. Results

The band structure and partial densities of states were calculated for Cd-M alloys with hcp structure using a unit cell with 15 Cd atoms and one impurity atom, i.e. the point impurity system is simulated by a $Cd_{15}M$ alloy. The unit cell for $Cd_{15}M$ is shown in Figure 1. The usual unit cell for Cd metal with hexagonal basis vectors $\boldsymbol{a}_1$, $\boldsymbol{a}_2$, and $\boldsymbol{c}$ is shown in thick lines. The 16 atoms of the supercell are labeled A-F. F is the impurity atom, and equivalent Cd atoms are labeled by the same letter.

The upper part of Fig. 2 shows the band structure of pure Cd metal folded into the Brillouin zone of the supercell (Cd_{16}); the band structure for $Cd_{15}In$ is shown in the lower part. In the latter the lowest lying bands are the 4 d-bands of In. These bands are by about 4 eV below the 4 d-bands of Cd. The 4 d-bands of Cd partly overlap the 5 sp-valence bands (For $Cd_{15}Xe$ the 5 s band of Xe is lying below the 4 d-bands of Cd). The 5 sp-valence bands are multiply degenerate for Cd_{16} because of the folding. These artificial degeneracies are lifted in $Cd_{15}In$.

To get some insight in the influence of the impurity atom on the charge distribution of the various Cd neighbors the total charge Q_v, (13), is listed in Table 1 for the systems $Cd_{15}M$, M = In, ..., Xe. One sees that

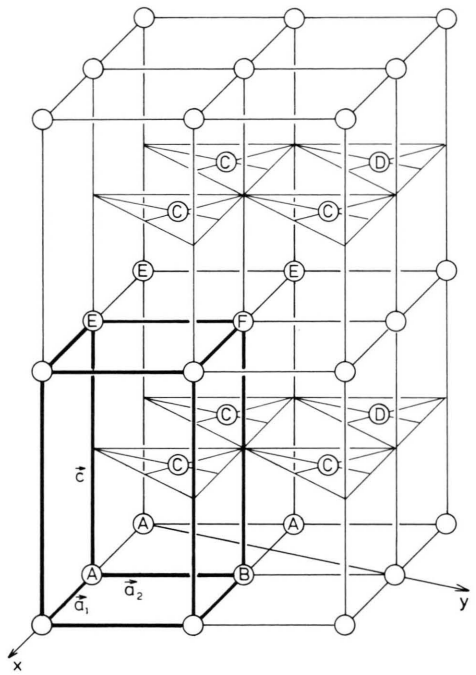

Fig. 1. Hcp unit cell with 16 atoms per unit cell. The regular hcp unit cell with unit vectors $\boldsymbol{a}_1$, $\boldsymbol{a}_2$, and $\boldsymbol{c}$ is drawn in thick lines. F is the position of the impurity atom M in $Cd_{15}M$. Equivalent positions of the 15 Cd atoms are labeled by the same letter.

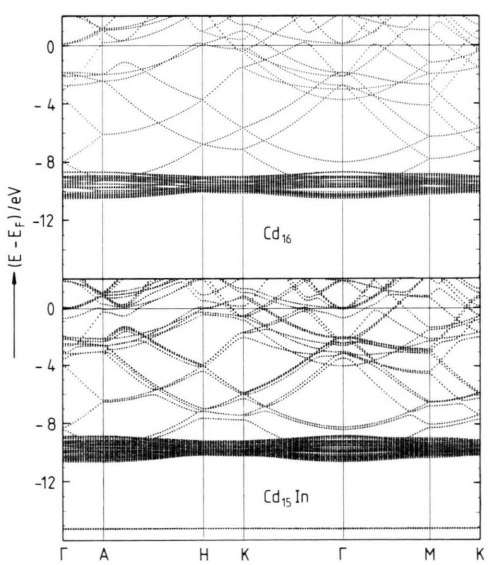

Fig. 2. Band structures of Cd_{16} and $Cd_{15}In$. E_F is the Fermi energy.

Table 1. Electronic charge Q_ν of the valence electrons inside the atomic sheres of radii 1.714 Å in $Cd_{15}M$, M = In, Sn, Sb, I and Xe. For pure Cd $Q_{Cd} = 2e^-$. The atoms are labeled as shown in Fig. 1. F is the impurity atom M, E is the nearest neighbor, C the next nearest neighbor etc.

	$Cd_{15}In$	$Cd_{15}Sn$	$Cd_{15}Sb$	$Cd_{15}I$	$Cd_{15}Xe$
F	2.891	3.762	4.724	6.719	7.522
E	2.019	2.054	2.064	2.069	2.107
C	2.008	2.016	2.013	2.014	2.027
D	2.001	2.007	2.002	2.004	2.007
B	2.005	1.999	2.003	2.002	1.989
A	1.998	1.999	1.999	1.994	1.997

only the total charges of the nearest and next nearest neighbors are influenced distinctly by the charge of the impurity atom. Considering the delocalized Bloch functions one finds larger amplitudes in the region of the impurity atoms than in the rest of the lattice (Cd atoms), see also the partial charges in Fig. 4 (the 5 s electrons of Xe, however, form non bonding states below the 4 d levels of Cd). The change in the number of valence electrons per unit cell for $Cd_{15}M$ compared to Cd_{16} gives rise to occupied electron states at the Fermi level E_F which are previously not occupied in the case of pure cadmium, see Figure 2.

Figure 3 a shows the density of states $N(E)$ for pure Cd metal. Only the energy range of the valence electrons is displayed. For low energy values $N(E)$ shows a free electron like increase. However a distinct minimum of $N(E)$ exists near E_F (see also [12]). For $Cd_{15}In$ the quantity $N(E)$ shows the same behavior. The Fermi energy, however, is shifted towards the minimum of the density of states. For the systems with non-metal impurity atoms the density of states shows more structure.

The p-partial densities of states are given in the lower part of Figure 3. For low energy values $N_{v=Cd,\,p_x}(E) = N_{Cd,\,p_y}(E) > N_{Cd,\,p_z}(E)$. For the corresponding one-electron wave functions of a general $\boldsymbol{k}$-point the p_x amplitudes (the $|a^{(\nu)}_{L,i}|$ in (6)) are larger than the p_z ones. This is a well-known behavior for hcp metals like Cd for which the c/a ratio is larger than the ideal value of 1.633. With increasing E, $N_{v,\,p_x}(E)$ follows the shape of the total density of states with a minimum close to E_F. For $N_{v,\,p_z}$ this minimum does not exist because in the energy range near E_F the p_z-amplitudes become larger than for low energy values. It follows that $N_{v,\,p_x}(E)$ intersects $N_{v,\,p_z}(E)$ for E near E_F.

Next we consider the integrals over $N_{v,\,p_j}(E)$, i.e. the charges $Q_{v,\,p_j}(E)$. The two lowest curves in the upper

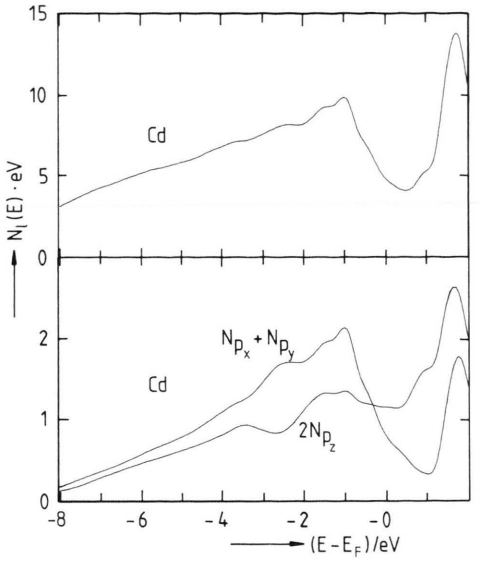

Fig. 3. Density of states $N(E)$ and partial p-density of states N_p for Cd metal.

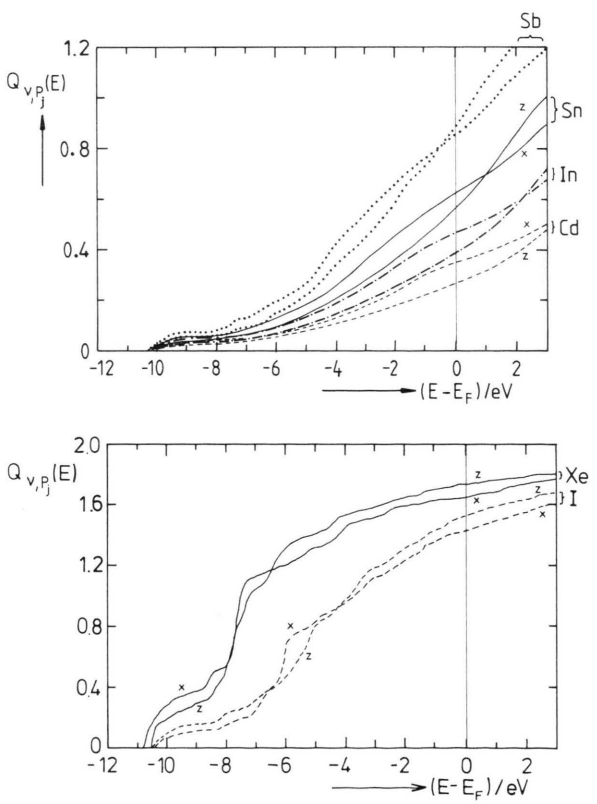

Fig. 4. Partial charges $Q_{v,\,p_j}(E)$ vs. E, (14), for atoms in $Cd_{15}M$, M = Cd, . . . , Xe.

part of Fig. 4 are the results for $Q_{v,p_x}(E)$ and $Q_{v,p_z}(E)$ for Cd in Cd metal. These curves are the same for Cd at the position A (Fig. 1) in $Cd_{15}M$. As expected from the shape of the $N_{v,p_j}(E)$ curves in Fig. 3 $Q_{v,p_x}(E)$ is larger than $Q_{v,p_z}(E)$. The difference

$$\Delta Q_{v,p}(E) = Q_{v,p_x}(E) - Q_{v,p_z}(E) \tag{17}$$

has its maximum for the energy value of the intersection of $N_{v,p_x}(E)$ and $N_{v,p_z}(E)$ in Figure 3. Beyond this energy value $Q_{v,p_x}(E)$ and $Q_{v,p_z}(E)$ approach each other. For Cd the intersection point E_c, for which $Q_{v,p_x}(E_c) = Q_{v,p_z}(E_c)$, is beyond the energy range displayed in Figure 4.

For the impurity atoms the intersection point E_c is shifted to lower energies and the shift is increasing with increasing atomic number of the impurity atom, see Fig. 4, and $\Delta Q_{v,p}(E_F)$ changes sign going from $Cd_{15}Sn$ to $Cd_{15}Sb$. From Fig. 4 one again sees that the extra charge of the impurity atoms compared to Cd is mainly localized at the impurity atom, as the partial charges $Q_{v,L}(E)$ are continously increasing with increasing number of valence electrons of the impurity atom.

Furthermore, the sign reversal of $\Delta Q_{v,p}(E_F)$, and with it the sign reversal of the EFG (see (15)), cannot be explained by the rigid band model on the basis of the band structure of Cd. Assuming that the main effect of the impurity is the filling up of electronic states of the host metal the Fermi energy would increase by 1.5 eV going from Cd_{16} to $Cd_{15}Xe$. Within the rigid band model $\Delta Q_{v,p}(E_F)$ is still positive for $Cd_{15}Xe$, see the Cd curves in Figure 4.

We finally turn to a discussion of the EFG. To use (15) the expectation values $\langle r^{-3}\rangle_v$ must be known. These $\langle r^{-3}\rangle_v$ values are deduced from a relativistic atomic calculation using the local density-functional approach [13] and taking into account the normalization given above. The results for the EFG are given in Table 2 together with the experimental values. One sees that the calculated values for the EFG give the right trend. From these results the increase of $q^{(In)}$ compared to $q^{(Cd)}$ is mainly caused by the difference in the atomic radial 5 *p* wave functions of the two atoms. The increase of $q^{(Sn)}$ compared to $q^{(In)}$ could not be reproduced by these calculation as the increase of $\langle r^{-3}\rangle_{Sn}$ compared to $\langle r^{-3}\rangle_{In}$ is smaller than the decrease of the corresponding $\Delta Q_{v,p}(E_F)$ values. The calculated values for $q^{(Sb)}$ and $q^{(I)}$ are quite satisfactory. However, the increase of the EFG for Xe compared to *I* found theoretically is smaller than the experimental results. The reasons for the quantitative differences between the experimental and theoretical values for the EFG are discussed in the next section.

Table 2. Electric field gradient (in 10^{17} V/cm^2) in cadmium-based alloys Cd-M at the impurity site. $\Delta Q_v(E_F)$ is the difference in the p-like charges, (17), $\langle r^{-3}\rangle_v$ is the expectation value of r^{-3} for an atomic 5 p wave function normalized to the Wigner-Seitz sphere ([a] Ref. 3; * Sign not given).

M	$\Delta Q_M(E_F)$	$\langle r^{-3}\rangle_M$	Electric field gradient	
			Eq. (11)	Exp[a]
Cd	0.084	11.43	7.47	+ 7.2
In	0.082	14.64	9.34	+ 10.7
Sn	0.056	16.21	7.06	+ 11.0
Sb	− 0.010	17.99	− 0.70	0.4*
I	− 0.098	23.05	− 8.79	− 16.8
Xe	− 0.080	26.15	− 8.14	6.2*

4. Discussion

Let us first discuss the reasons for the differences between the experimental and theoretical values for the EFG. As pointed out in Sect. 2, only the valence electron contributions originating from the *p*-like charge of the electronic states were calculated. Summing over all (L, L'), i.e. calculating the total electronic contribution with (7), from the ASW wave functions one gets $q_{v,d} = 6.6 \cdot 10^{17}$ V/cm^2. This value is smaller than the value given in Table 2; this is understandable as the non *p*-*p* components in (7) like $q_i(L = 0, 0)$, $L' = (2, 0)$) give a net negative contribution to the EFG. For computer time reasons the values for the EFG on the basis of (7) could not yet be calculated for the systems with the impurity atoms. Another source of error is the omission of core contributions, as discussed in Section 2. Furthermore, the crystal potential for the self-consistent procedure was approximated by a spherically symmetric one, and therefore the hcp symmetry is only included by the structure factors of the wave functions. Also the lattice distortion by the impurity atom was not taken into account. On the other side, the uncertainty in the knowledge of the nuclear quadrupole moment to determine the experimental EFG must be taken into consideration, too. It seems, however, that all these contributions only influence the magnitudes of the EFG at the nucleus site of the impurity whereas the general trend is given by the *difference* of p_j-like charge distributions for the point impurities.

Secondly, comparing the band structure results with the molecular orbital investigations [3, 4] it follows that the density of states and partial densities of states deduced from first principles (Fig. 3–4) do not agree with the model assumptions (gaussian and free electron like, see Section 1). However, the conclusion that the trend in the EFG in the Cd-M system can be explained on the basis of the finding that for the hcp point symmetry with c/a larger than the ideal ratio p_x, p_y like electronic states are energetically favored compared to the p_z like ones is the same in the present and in earlier [3, 4] investigations.

Acknowledgement

We are grateful to the Deutsche Forschungsgemeinschaft for support of this work.

[1] E. N. Kaufmann and R. J. Vianden, Rev. Mod. Phys. **51,** 161 (1979).
[2] T. P. Das and P. C. Schmidt, Z. Naturforsch. **41 a,** 47 (1986).
[3] H. Haas, Z. Naturforsch. **41 a,** 78 (1986).
[4] B. Lindgren, Phys. Rev. **B 34,** 648 (1986).
[5] R. M. Sternheimer, Phys. Rev. **130,** 1423 (1963); **132,** 1637 (1963) and Z. Naturforsch. **41 a,** 24 (1986); P. C. Schmidt, K. D. Sen, Alarich Weiss, and T. P. Das, Phys. Rev. **B 22,** 4167 (1980).
[6] H. M. Foley, R. M. Sternheimer, and D. Tycko, Phys. Rev. **93,** 734 (1954); R. Sternheimer, Phys. Rev. **146,** 140 (1966); E. H. Hygh and T. P. Das, Phys. Rev. **143,** 452 (1966); P. C. Pattnaik, M. D. Thompson, and T. P. Das, Phys. Rev. **B 16,** 5390 (1977); K. K. P. Rao and N. C. Mohapatra, Phys. Rev. **A 24,** 10 (1981); K. D. Sen, P. C. Schmidt, and Alarich Weiss, Z. Naturforsch. **41 a,** 37 (1986).
[7] T. P. Das and M. Pomerantz, Phys. Rev. **123,** 2070 (1961).
[8] M. D. Thompson, Ph.D. Thesis, State University of New York at Albany 1979 (unpublished); M. D. Thompson, G. Ciobanu, and T. P. Das, to be published.
[9] P. Blaha, K. Schwarz, and P. H. Dederichs, to be published.
[10] A. R. Williams, J. Kübler, and C. D. Gelatt, Jr. Phys. Rev. **B 19,** 6094 (1979).
[11] T. P. Das and E. L. Hahn, Nuclear Quadrupole Resonance Spectroscopy, Academic Press, New York 1957.
[12] R. V. Kasowski, Phys. Rev. **187,** 891 (1969).
[13] P. Hohenberg and W. Kohn, Phys. Rev. **136,** B 864 (1964); W. Kohn and L. J. Sham, Phys. Rev. **140,** A 1133 (1965); A. H. Mac Donald and S. H. Vosko, J. Phys. **C 12,** 2977 (1979).